Journal of Solid State Chemistry 182 (2009) 1679–1684

Contents lists available at ScienceDirect

Journal of Solid State Chemistry

journal homepage: www.elsevier.com/locate/jssc

A conversion route towards tubular SiO_2 using rod-like $BaSiF_6$ as a novel template

Hao-Xiang Zhong [a], Qing-Li Huang [a], Ying-Li Ma [a], Jian-Ming Hong [b], Xue-Tai Chen [a,*], Zi-Ling Xue [c]

[a] Coordination Chemistry Institute, State Key Laboratory of Coordination Chemistry, Nanjing National Laboratory of Microstructures, School of Chemistry and Chemical Engineering, Nanjing University, Nanjing 210093, PR China
[b] Analytic Center of Nanjing University, Jiangsu, Nanjing 210093, PR China
[c] Department of Chemistry, University of Tennessee, Knoxville, Tennessee 37996-1600, USA

ARTICLE INFO

Article history:
Received 21 January 2009
Received in revised form
26 March 2009
Accepted 28 March 2009
Available online 16 April 2009

Keywords:
Template synthesis
$BaSiF_6$
Tubular silica
Hydrothermal synthesis.

ABSTRACT

A simple hydrothermal reaction between $Ba(NO_3)_2$ and K_2SiF_6 results in the formation of 1D rod-like $BaSiF_6$. The $BaSiF_6$ rods can act as efficient precursors for production of tubular SiO_2 by hydrothermal reaction in alkaline solutions. Powder X-ray diffraction (XRD), X-ray photoelectron spectra (XPS), transmission electron microscopy (TEM), high resolution electron microscopy (HRTEM), and field emission scanning electron microscopy (FESEM) were used to characterize the phase and morphology of the final product. The experiments indicated the amount of NaOH, reaction temperature, and reaction time played important roles in the transformation process. A possible growth mechanism of tubular silica was proposed.

1. Introduction

Recently, much research effort has been devoted to the design and synthesis of tubular materials since the first discovery of carbon nanotubes [1]. Up to now, various tubular structures such as metals (Au [2] and Te [3]), sulfides [4], nitrides [5] and oxides (SiO_2 [6], ZnO [7], TiO_2 [8], VO_x [9], and CeO_2 [10]) have been fabricated. Amongst the oxide systems, silica has attracted particular attention because of their potential applications as a catalyst support material [11], as a core material for biosensors and biomarkers [12], as storage/delivery containers for biochemical substances [13] and in optoelectronic nanodevice design [14,15]. Two synthetic approaches to silica nanotubes have been reported, namely, template approach [16] and direct chemical/physical routes [17,18]. As a representative synthetic method, several templates have been developed for the synthesis of tubular SiO_2, such as surfactant [19], organogelators [20,21], biological substrates [22], organic ammounium carboxylate crystals [23], nanoporous membrane materials [24,25], carbon nanotubes [26,27], fiber-like crystals of $[Pt(NH_3)_4](HCO_3)_2$ [28], ZnS [29], $V_3O_7 \cdot H_2O$ [30] and so on. However to the best of our knowledge, most reported templates for the preparation of tubular SiO_2 only act as a physical template to control the size and morphology of the final product and contain nothing of the chemical composition of the desired product. Herein, we report on the synthesis of the tubular SiO_2 in alkaline solutions by employing rod-like $BaSiF_6$ as both the physical and chemical templates. No other additive was used in the current synthesis. The advantage of using such physical/chemical template is that the final removal of the template is not required since the template has been sacrificed. Another benefit is the ease control of the composition of the final material.

2. Experimental details

2.1. Synthesis of $BaSiF_6$ precursor

All chemical reagents used in this study were of analytical grade. $Ba(NO_3)_2$ (0.1 mol/L, 10 mL) and K_2SiF_6 (0.1 mol/L, 10 mL) were mixed and stirred for 10 min. Then the mixture solution was transferred into a 30 mL stainless Teflon-lined autoclave and heated at 120 °C for 6 h. The powder samples obtained were centrifuged, washed with distilled water, and dried at 60 °C.

2.2. Synthesis of tubular SiO_2

The $BaSiF_6$ precursor (0.54 mmol) was dispersed into distilled water (25 mL). After the addition of NaOH (1.80 mmol), and stirred for 10 min, the mixture was transferred into a 30 mL stainless

* Corresponding author. Fax: +86 25 83314502.
E-mail address: xtchen@netra.nju.edu.cn (X.-T. Chen).

0022-4596/$ - see front matter © 2009 Elsevier Inc. All rights reserved.
doi:10.1016/j.jssc.2009.03.037

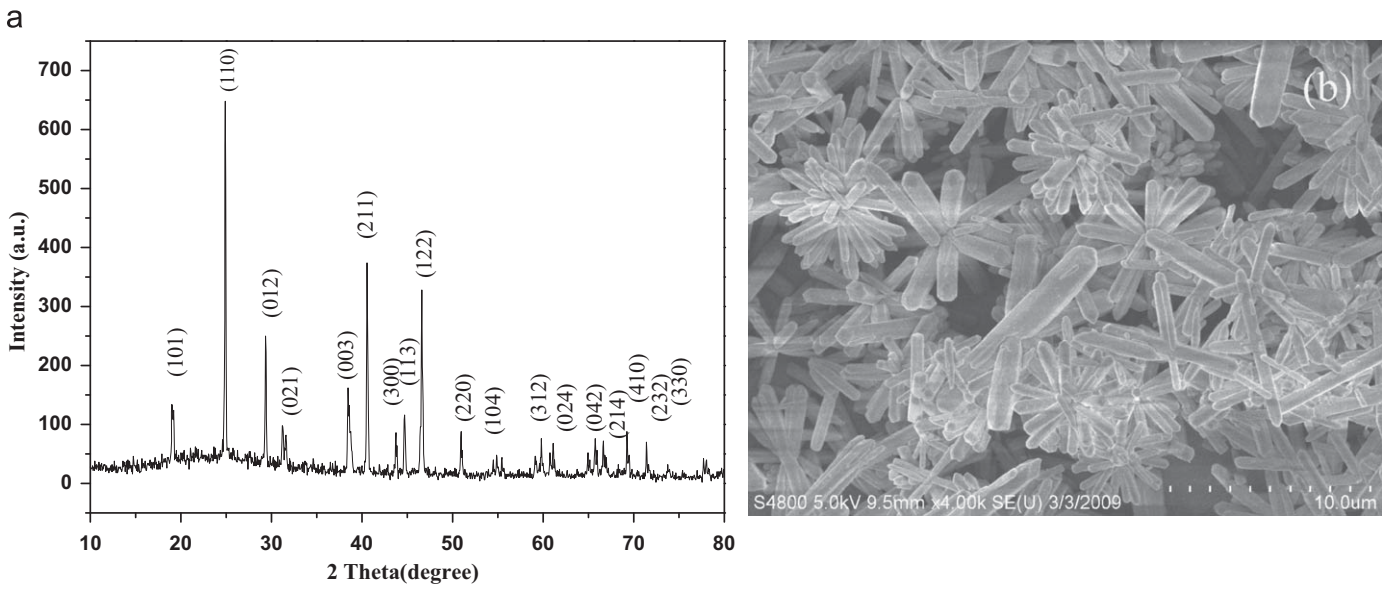

Fig. 1. (a) XRD and (b) SEM patterns of the as-prepared $BaSiF_6$.

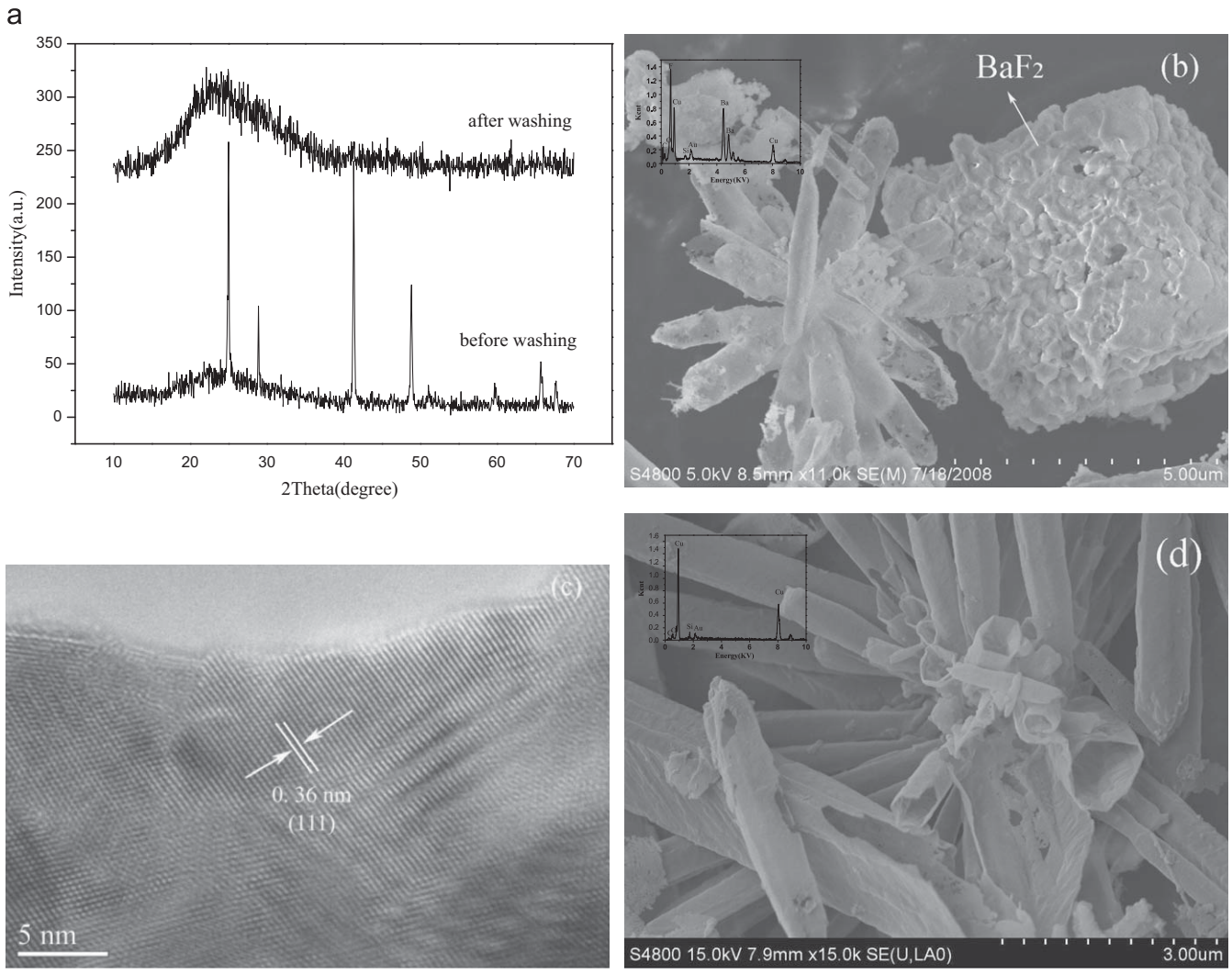

Fig. 2. (a) XRD of the product before and after washing; (b and c) SEM, and HRTEM images of the product before washing (inset, EDS); (d–g) TEM, SEM, and HRTEM images of the product after washing (inset, EDS, ED); (h) XPS spectrum of the tube after washing.

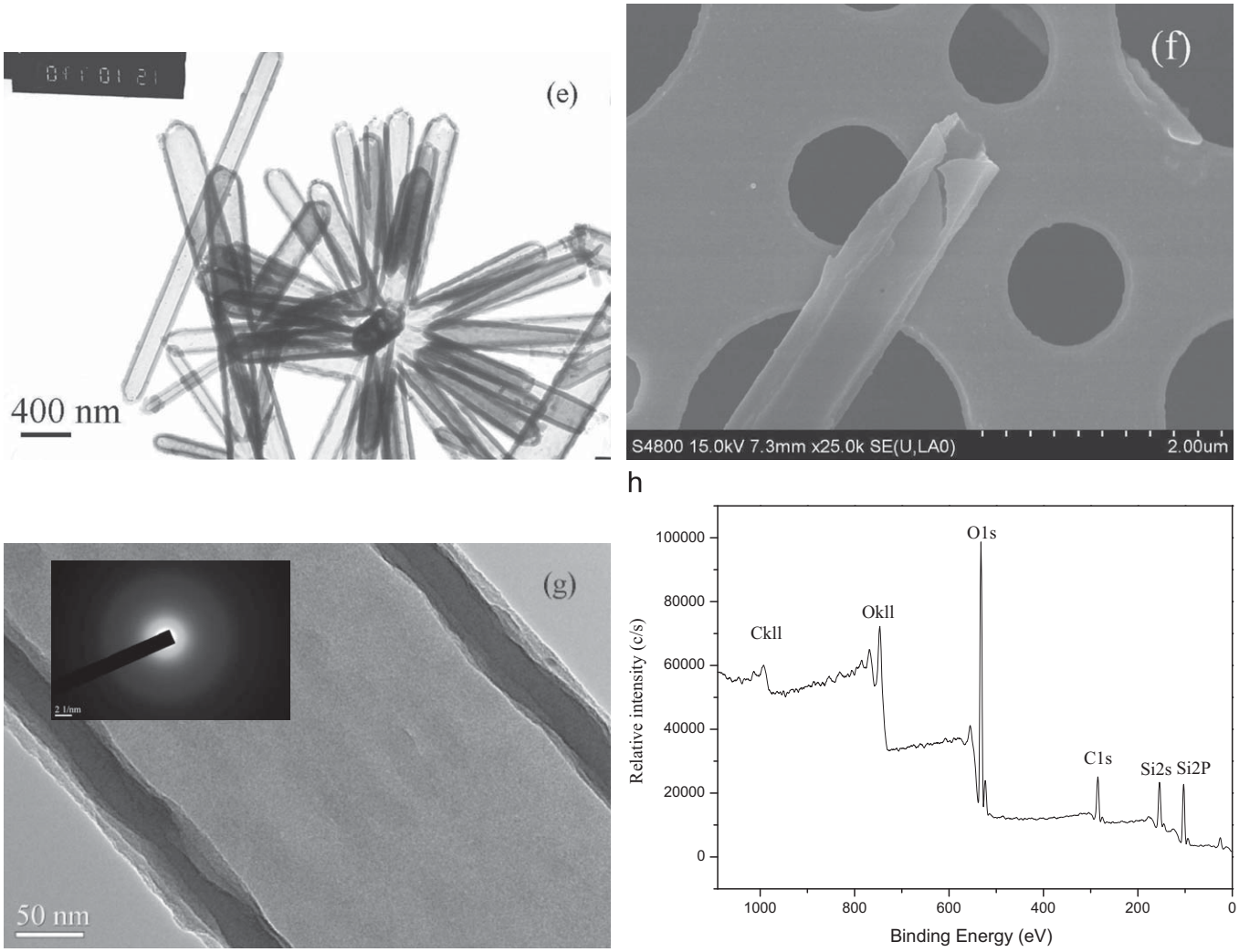

Fig. 2. (*Continued*)

Teflon-lined autoclave and heated at 120 °C for 6 h. The samples were collected, washed several times with distilled water, and dried at 60 °C for 4 h. A mixture of BaF_2 and SiO_2 was obtained. To obtain pure SiO_2, an acid treatment was employed to remove BaF_2. The mixture of BaF_2 and SiO_2 was added directly into 1.5 mol/L HNO_3 solution, and then were stirred for about 3 h. The solid sample obtained was washed several times with water, and dried at 60 °C for 4 h.

2.3. Characterizations

The crystalline phases of the products were analyzed by X-ray diffraction (XRD) on a Shimadzu XRD-6000 powder X-ray diffractometer (Cu$K\alpha$ radiation $\lambda = 1.5418$ Å) at a scanning rate of $0.05^\circ s^{-1}$ in the 2θ range 10–70°. The X-ray photoelectron spectra (XPS) were recorded on an ESCALAB MK II X-ray photoelectron spectrometer, using Mg K-X-ray as the excitation source. The sizes and morphologies of the products were studied by field emission scanning electron microscopy (FESEM, HITACHI-S4800), transmission electron microscopy (TEM, TECNAI-12), and high resolution electron microscopy (HRTEM, JEM-2010). X-ray fluorescence (XRF) analysis was performed on an ARL-9800 spectrometer.

3. Results and discussion

3.1. Synthesis and characterizations

The direct reaction between $Ba(NO_3)_2$ and K_2SiF_6 readily generates rod-like $BaSiF_6$ with a high yield. The XRD pattern of the precursor $BaSiF_6$ is shown in Fig. 1a. All peaks can be indexed to a pure rhombohedral phase (space group: $R\bar{3}m$, with lattice constant $a = 7.198$ Å, $c = 7.020$ Å; JCPDS 78-0031). No other impurity peaks are detected in the XRD pattern. Fig. 1b shows a typical SEM image of the product, from which many rods with lengths up to several micrometers and diameters around 300–500 nm can be clearly found.

It was expected that the rod-like $BaSiF_6$ could act as the precursor and/or template to generate the 1D nano/micro-structures of Ba- or Si-containing material. Because $BaSiF_6$ is unstable in alkaline solutions, the precursor can be treated with basic solution to obtain pure SiO_2. When $BaSiF_6$ was reacted with ca. 3 molar equivalence of NaOH via a simple hydrothermal procedure, and then followed by the removal of the produced BaF_2 through acid treatment, the pure SiO_2 tubes were obtained. Fig. 2a shows the XRD patterns of the products prepared by the hydrothermal process before and after the acid treatment, respectively. Before washing with acid, it is found that the

product can be indexed to a cubic BaF_2 phase (space group: $Fm3m$), which is consistent with the values in the standard cards (JCPDS Card no. 04–0452). But after the acid treatment, only a broad peak at $2\theta = 20–30^\circ$ was found in the XRD pattern, which indicated the amorphous nature of the product. The above experimental results imply that the product before washing is the mixture of BaF_2 and the amorphous SiO_2. Since the diffraction peaks of BaF_2 in the mixed product are very strong, the halo peak of amorphous SiO_2 could not be seen in the diffraction pattern of the mixed product.

Fig. 2b shows the typical SEM images of the mixture product before treating with acid. There are many irregular particles or aggregates along with SiO_2 tubes. The EDS of these irregular particles confirmed that main chemical composition is BaF_2 (inset, Fig. 2b). The HRTEM image of a region of an irregular particle shows it is structurally uniform with interplanar spacing of about 0.36 nm, which corresponds to the (111) lattice spacing of BaF_2 (Fig. 2c). Therefore, the identity of these irregular particles was demonstrated to be BaF_2 by HRTEM and EDS. The images of the products after treating with acid were shown in Figs. 2d–g. The flower-like SiO_2 microstructures consisted of SiO_2 tubes could be clearly found from the images in Figs. 2d and e. A tip of a cracked SiO_2 tube clearly shows a hollow interior of tubular structure with diameters in the range of 300–400 nm, and shell thickness less than 60 nm (Fig. 2f). These are further confirmed by the HRTEM image of a single SiO_2 tube (Fig. 2g). No lattice fringe could be observed for the tubular SiO_2, indicating it is in the amorphous state. The corresponding selected-area electron diffraction (SAED) pattern (inset, Fig. 2g) shows only diffuse rings without diffraction spots, which further confirm its amorphous nature. The corresponding elemental composition is confirmed by EDS (inset, Fig. 2d) to be Si and O with an approximate atomic ratio of 1:2 (the Cu signal comes from the copper grids.), indicating that these tubes are amorphous SiO_2. No obvious peak of other element such as Ba is detected. XRF data of the product indicated that only 0.3 atm% Ba existed, which demonstrated that nearly all of the BaF_2 produced along with SiO_2 was washed away by treating with HNO_3 for 3 h. The surface composition of the amorphous SiO_2 was further probed by XPS (Fig. 2h). The relatively strong peaks at 154.5, 103.0, and 532.5 eV can be attributed to the bonding energies of Si_{2s}, Si_{2p}, and O_{1s}, respectively. These results are in agreement with those reported [15,31]. No obvious peaks for Ba or F were observed besides C peaks from the XPS chamber.

The above observations showed that the rod-like $BaSiF_6$ could be transformed into a mixture of BaF_2 and SiO_2. After treating with acid, tubular SiO_2 was prepared. XRD and TEM were carried out on the products isolated at different reaction stages to investigate the factors involved in the transformation process

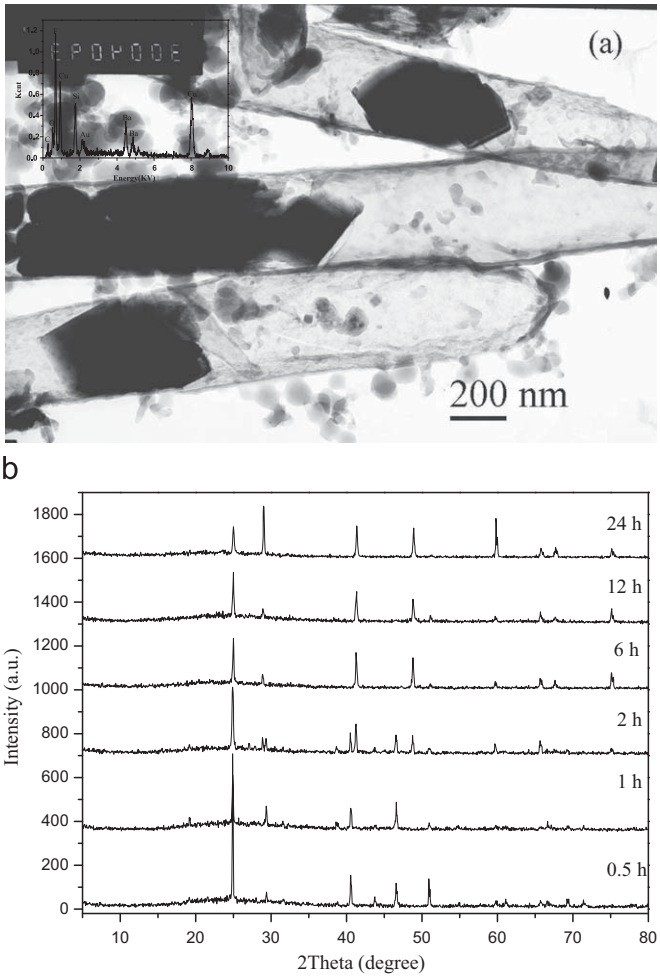

Fig. 3. (a) TEM images of the products correspond to reaction stages at 2.0 h (inset, EDS) and (b) XRD patterns of the products obtained at reaction stages of 0.5, 1.0, 2.0, 6.0, 12.0, and 24.0 h, respectively.

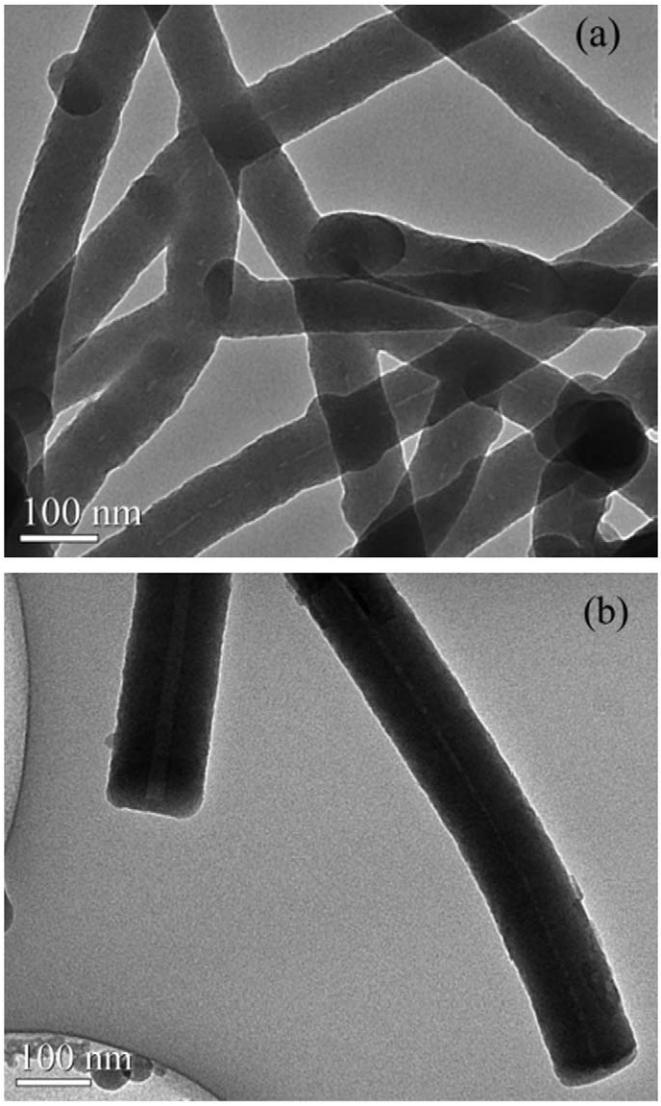

Fig. 4. (a and b) SEM images of the product obtained with 2.3 mmol NaOH at 120 °C for 6 h after washing with acid.

and the formation of the tubular SiO_2. When the reaction time was shortened to 0.5 h, only random rods with a diameter around 300–500 nm were observed. The X-ray diffraction pattern of the product showed that it was pure $BaSiF_6$ with the rhombohedral structure (Fig. 3b). Increasing reaction time up to 1 h, the rods and a small quantity of tubes coexisted. The X-ray diffraction pattern of the product is mainly the rhombohedral $BaSiF_6$ (Fig. 3b). When the reaction time reaches at 2.0 h, the images in Fig. 3a showed that the partially filled rods or partial tubes were found. It appears that the tubular structures were formed from the erosion of the template starting at the tips of the rod. EDS (inset, Fig. 3a) of the partial tube shows the Ba, Si, F, and O elements coexisted, and the amount of Si is much more than that of Ba. The X-ray diffraction pattern of the product obtained at this stage showed the mixed phases of the cubic BaF_2 and $BaSiF_6$. When the reaction time was further prolonged to 6 h (Fig. 2b), the mixed morphologies of tubes and irregular particles coexisted. The X-ray diffraction pattern of the product showed that the only cubic BaF_2 existed, indicating that $BaSiF_6$ was completely transformed into BaF_2 and SiO_2 (Fig. 2a). Because SiO_2 is amorphous in nature, only those diffraction peaks of BaF_2 were observed. When the reaction was further prolonged (12, 24 h), the product still preserved the tubular morphology. It can be deduced that the formation of tubular SiO_2 involves three steps. First, the precursors $BaSiF_6$ nanorods formed. Second, the precursor is reacted with NaOH to yield a mixture of SiO_2 and BaF_2. Finally, BaF_2 is removed by acid treatment, which results in the final hollow morphology.

The following reactions occur in the formation of tubular SiO_2:

$$Ba^{2+} + SiF_6^{2-} \rightarrow BaSiF_6 \downarrow \quad (1)$$

$$BaSiF_6 + 4OH^- \rightarrow BaF_2 \downarrow + SiO_2 + 4F + 2H_2O \quad (2)$$

It has been found that the amount of alkaline have great influence on the products. When the amount of NaOH was less than 1.5 mmol, the $BaSiF_6$ rods did not completely transform into the mixture of BaF_2 and SiO_2. When the amount of NaOH was increased to 1.8 mmol, a mixture of BaF_2 and SiO_2 was produced, and the tubular SiO_2 was obtained after acid washing. Further increasing the amount of NaOH to 2.3 mmol, the SiO_2 tubes with the diameter of 50 nm were produced after washing with acid (Fig. 4a). It should be noted that the size of this tubular product is much smaller than that of the precursor $BaSiF_6$. Only irregular small sphere were obtained with 5 mmol NaOH.

The reaction temperature was also found to affect the transformation. At a low temperature such as 80 °C, the product was still $BaSiF_6$ rods. When temperature was raised to 120 °C, SiO_2 tubes were produced after washing with acid (Figs. 2e–h). Further increasing the temperature to 160 °C, the bamboo-like tubes of SiO_2 were obtained after washing the mixture (Figs. 5a and b). When the temperature was further raised to 180 °C, SiO_2 with the long bamboo-like tubes were still kept after washing the mixture with acid.

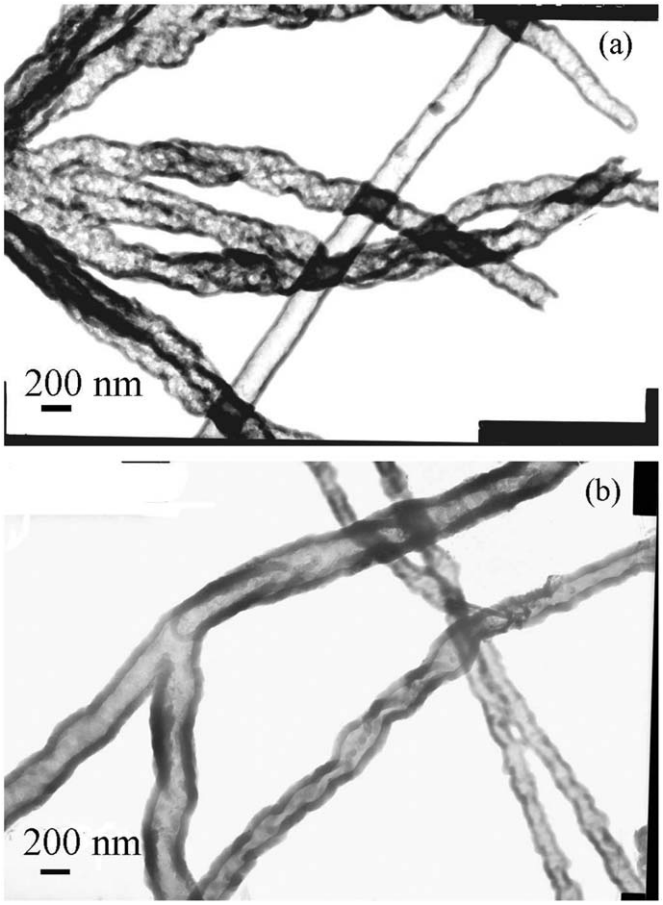

Fig. 5. TEM images of the products obtained at different temperature (a and b) 160 °C, 6 h, after washing.

3.2. Growth mechanism

On the basis of all the above observations, a template-based growth mechanism of the straight silica tube is proposed. The above findings suggest that the three-stage processes are responsible for the formation of the tubular silica. The possible formation mechanism of SiO_2 was illustrated in Scheme 1. $BaSiF_6$ rods were formed first, which might be due to the anisotropical nature of crystal structure and intrinsic growth characteristics. The TEM image of the product obtained after reaction for 2 h shown in Fig. 3a clearly suggest that the erosion started on both ends. Therefore it is reasonable to assume that the reactivity rates of the different crystalline planes were significantly varied due to the different surface energies when $BaSiF_6$ was treated with NaOH. Two ends of $BaSiF_6$ rod reacted with NaOH much faster than the side surfaces. Therefore the erosion of the $BaSiF_6$ first occurred on the two tips, yielding the primary SiO_2 and BaF_2 particles. At the same time, these produced SiO_2 particles could coat on the exterior surface of $BaSiF_6$ while the produced BaF_2 remained in the hole or the solution. With the increasing of the

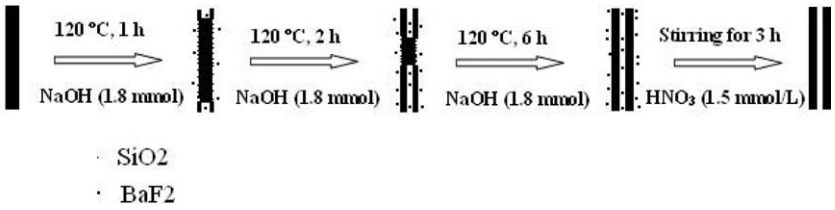

Scheme 1. Schematic illustration of the tubular silica formation.

reaction time, the interior was gradually hollow and the silica sheath was developed. When the $BaSiF_6$ was completely consumed, the mixture of SiO_2 tubes and BaF_2 particles were formed. The final removal of BaF_2 led to the pure tubular SiO_2. Therefore, in this formation process of silica tubes, $BaSiF_6$ rods both served as the precursor and the template. The different reactivity of crystalline planes of $BaSiF_6$ rods with NaOH was assumed to essential for the formation of silica tubes. The optimal reaction condition for silica tubes was the addition of 1.8 mmol NaOH with respect to 0.54 mmol $BaSiF_6$.

With the excess of NaOH (e.g. 2.3 mmol NaOH), part of the NaOH would react with the ends of $BaSiF_6$ first, the remaining NaOH would also react with the lateral surfaces of $BaSiF_6$. When the erosion on the different directions occur at comparable rate, which lead to the SiO_2 tubes with smaller diameter. With much more NaOH was used, (i.e. 5 mmol NaOH), the erosions on both ends and the lateral surfaces are very fast, which would destroy the template, leading to the formation of irregular particles.

4. Conclusions

In summary, we have successfully fabricated tubular SiO_2 and rod-like BaF_2 by using $BaSiF_6$ nanorods as precursors. The hydrothermal treatment of $BaSiF_6$ with a certain amount of NaOH at a mild temperature (120 °C) produces SiO_2 tubes. The reaction parameters such as reaction time, temperature, and the amount of NaOH were studied to investigate the factors involved in the solid–liquid interface reactions of $BaSiF_6$ to SiO_2. $BaSiF_6$ nanorods not only act as the precursor but also serve as chemical/physical templates, which lead to the formation of SiO_2 tubes. This method may be extended to the preparation of other oxides.

Acknowledgments

This work was supported by National Basic Research Program of China (nos. 2006CB806104 and 2007CB925102 to XC), Natural Science Grant of China (no. 50572037 to XC), and US National Science Foundation (to ZX).

References

[1] S. Iijima, Nature 354 (1991) 56–58.
[2] Y. Sun, B.T. Mayers, Y. Xia, Nano Lett. 2 (2002) 481–485.
[3] W.H. Xu, J.M. Song, L. Sun, J.L. Yang, W.P. Hu, Z.Y. Ji, S.H. Yu, Cryst. Growth Des. 4 (2008) 888–893.
[4] Y. Feldman, E. Wasserman, D. Tenne, R. Srolovitz, Science 267 (1995) 222–225.
[5] S. Ding, P. Lu, J.G. Zheng, X.F. Yang, F.L. Zhao, J. Chen, H. Wu, M.M. Wu, Adv. Funct. Mater. 17 (2007) 1879–1886.
[6] G. Shen, Y. Bando, D. Golberg, J. Phys. Chem. B 110 (2006) 23170–23174.
[7] L. Shen, N. Bao, K. Yanagisawa, K. Domen, C.A. Grimes, A. Gupta, J. Phys. Chem. C 111 (2007) 7280–7287.
[8] D.X. Liu, M.Z. Yates, Langmuir 23 (2007) 10333–10341.
[9] C. O'Dwyer, D. Navas, V. Lavayen, E. Benavente, M.A. Santa Ana, G. Gonzalez, S.B. Newcomb, C.M. Sotomayor Torres, Chem. Mater. 18 (2006) 3016–3022.
[10] G.Z. Chen, C.X. Xu, X.Y. Song, W. Zhao, Y. Ding, S.X. Sun, Inorg. Chem. 47 (2008) 723–728.
[11] A. Hanprasopwattana, S. Srinivasan, A.-G. Sault, A.-K. Datye, Langmuir 12 (1996) 3173–3179.
[12] M. Quobosheane, S. Santra, P. Zhang, W. Tan, Analyst 126 (2001) 1274–1278.
[13] T.K. Jain, I. Roy, T.K. De, A. Maitra, J. Am. Chem. Soc. 120 (1998) 11092–11095.
[14] H.J. Chang, Y.F. Chen, H.P. Lin, C.Y. Mou, Appl. Phys. Lett. 78 (2001) 3791–3793.
[15] M. Zhang, E. Ciocan, Y. Bando, K. Wada, L.L. Cheng, P. Pirouz, Appl. Phys. Lett. 80 (2002) 491–493.
[16] S. Hou, C.C. Harrell, L. Trofin, P. Kohli, C.R. Martin, J. Am. Chem. Soc. 126 (2004) 5674–5675.
[17] C.C. Tsai, H. Teng, Chem. Mater. 18 (2006) 367–373.
[18] L. Vayssieres, K. Keis, A. Hagfeldt, S.E. Lindquist, Chem. Mater. 13 (2001) 4395–4398.
[19] M. Harada, M. Adachi, Adv. Mater. 12 (2000) 839–841.
[20] S. Kobayashi, N. Hamasaki, M. Suzuki, M. Kimura, H. Shirai, K. Hanabusa, J. Am. Chem. Soc. 124 (2002) 6550–6551.
[21] J.H. Jung, S. Shinkai, T. Shimizu, Chem. Rec. 3 (2003) 212–224.
[22] W. Shenton, T. Douglas, M. Young, G. Stubbs, S. Mann, Adv. Mater. 11 (1999) 253–256.
[23] F. Miyaji, S.A. Davis, J.P.H. Charmant, S. Mann, Chem. Mater. 11 (1999) 3021–3024.
[24] A. Yamaguchi, H. Kaneda, W. Fu, N. Teramae, Adv. Mater. 20 (2008) 1034–1037.
[25] B.B. Lakshmi, C.J. Patrissi, C.R. Martin, Chem. Mater. 9 (1997) 2544–2550.
[26] C.N.R. Rao, B.C. Satishkumar, A. Govindaraj, Chem. Commun. (1997) 1581–1582.
[27] B.C. Satishkumar, A. Govindaraj, M. Nath, C.N.R. Rao, J. Mater. Chem. 10 (2000) 2115–2119.
[28] L. Ren, M. Wark, Chem. Mater. 17 (2005) 5928–5934.
[29] T.Y. Zhai, Z.J. Gu, Y. Dong, H.Z. Zhong, Y. Ma, H.B. Fu, Y.F. Li, J.N. Yao, J. Phys. Chem. C 111 (2007) 11604–11611.
[30] J. Zygmunt, F. Krumeich, R. Nesper, Adv. Mater. 15 (2003) 1538–1541.
[31] G.Z. Ran, L.P. You, L. Dai, Y.L. Liu, Y. Lv, X.S. Chen, G.G. Qin, Chem. Phys. Lett. 384 (2004) 94–97.